Optimizing Processing Conditions for Additively Reinforced Thermoforming (ART) in Convergent Manufacturing

Segun Isaac Talabi, Tyler Smith, Brittany Rodriguez, Ryan Ogle, Sana Elyas, David Nuttall, Vlastimil Kunc, Vipin Kumar, Ahmed Arabi Hassen

PII: S2352-4928(25)01382-0

DOI: https://doi.org/10.1016/j.mtcomm.2025.112870

Reference: MTCOMM112870

To appear in: *Materials Today Communications*

Received date: 26 February 2025
Revised date: 23 April 2025
Accepted date: 19 May 2025

Please cite this article as: Segun Isaac Talabi, Tyler Smith, Brittany Rodriguez, Ryan Ogle, Sana Elyas, David Nuttall, Vlastimil Kunc, Vipin Kumar and Ahmed Arabi Hassen, Optimizing Processing Conditions for Additively Reinforced Thermoforming (ART) in Convergent Manufacturing, *Materials Today Communications,* (2025) doi:https://doi.org/10.1016/j.mtcomm.2025.112870

Optimizing Processing Conditions for Additively Reinforced Thermoforming (ART) in Convergent Manufacturing

Segun Isaac Talabi[1], Tyler Smith[1], Brittany Rodriguez[1], Ryan Ogle[1], Sana Elyas[1], David Nuttall[1], Vlastimil Kunc[1], Vipin Kumar[1], Ahmed Arabi Hassen[1,*]

[1]Manufacturing Science Division, 2350 Cherahala Blvd, Oak Ridge National Laboratory, Oak Ridge, Knoxville, TN, 37932, USA

*_Corresponding authors_: A. A. Hassen, hassenaa@ornl.gov

Abstract

This study utilized additively reinforced thermoforming (ART) to enhance the thermomechanical properties of polyethylene terephthalate glycol (PETG) sheets. ART materials were produced by overprinting PETG/carbon fiber filament (PETG/CF) on neat PETG sheets at varying conditions. The mechanical properties of the PETG sheet, PETG/CF, and ART materials were assessed, showing that ART exhibited superior tensile strength and modulus of elasticity. The tensile strength and modulus in the x-direction for ART at 265°C were 57.32 ± 2.9 MPa and 3.41 ± 0.4 GPa, respectively, compared to 49.1 ± 0.5 MPa and 1.92 ± 0.09 GPa for neat PETG. Microstructural analysis revealed strong interfacial adhesion between layers, while thermogravimetric analysis (TGA), differential scanning calorimetry (DSC), and heat deflection temperature analysis provided insights into the ART material's thermoforming behavior, aiding design optimization for enhanced stiffness, reduced necking, and improved customization. This information can be used to design for the thermoforming operation.

Keywords: additive reinforcement, characterization, convergent manufacturing, polymer composite, thermoforming, thermoplastics.

1. Introduction

Thermoforming, a widely used manufacturing process, involves heating polymer sheets to a pliable temperature and shaping them using molds. This technique is valued for its efficiency in producing lightweight, durable components with complex geometries, making it integral to industries such as packaging, automotive, and consumer goods. In traditional thermoforming processes, polymer sheets like polyethylene terephthalate glycol (PETG) are commonly used due to their excellent formability, durability, and clarity [1-3]. However, bosses, snap-fits, inserts, or support structures such as ribs are often required to ensure structural integrity and achieve the desired geometrical stiffness [4]. This can be achieved through an overmolding process by injecting a complex feature directly onto the composite substrate for the purpose of structural or functional optimization [5, 6]. Although overmolding provides ability to incorporate such additional features, its high tooling costs and extended lead times limit its practicality to large-scale production runs. Moreover, due to the lack of flexibility of such support components, integration of additional features can only be done as a secondary operation. This limitation comes with increased complexity and costs [4]. Nowadays, thermoplastic composites are used due to their high strength-to-weight ratios, toughness, corrosion resistance, and recyclability [7-9].

In recent years, additive manufacturing (AM) has emerged as advanced manufacturing, transforming the production landscape across diverse industries [10]. One particularly impactful application of AM lies in the fabrication of reinforced polymer composites with control over the distribution and alignment of reinforcement within the final product [11]. This manufacturing technique can be adopted as a cost-effective alternative to overmolding via a concept referred to as overprinting. This method utilizes material extrusion processes to fabricate complex features directly onto sheets that will be used for thermoforming operations [12]. A novel system known as additive reinforced thermoforming (ART) takes this concept further by integrating AM with traditional thermoforming. The ART allows the precise reinforcement of polymer sheets using AM, which enhances their structural integrity. By tailoring reinforcement for different geometries and application, ART enhances the final product's performance while preserving the cost-efficiency and material versatility of traditional thermoforming. This represents a more efficient and sustainable solution. Recent studies have also shown that modifying PETG with nanofillers can significantly enhance its mechanical properties and functional capabilities, indicating further opportunities for material optimization in ART [13, 14]

ART presents an appealing proposition by merging the cost-efficiency of traditional composite manufacturing processes, such as thermoforming, with the design flexibility and material optimization of AM. This method enhances functionality, streamlines production, and supports shorter production cycles. It also enables the creation of tailored polymer sheets by directly printing various composites, providing precise control over performance characteristics. The additive, layer-by-layer process facilitates experimentation with reinforcement patterns and concentrations, ensuring adaptability to specific thermoforming needs. This innovation broadens the applications of polymers like PETG, enabling the development of multifunctional materials with optimized mechanical and thermal properties. Compared to other traditional reinforcement methods such as overmolding and fiber placement ART offered greater design flexibility, localized reinforcement control, and a more streamlined manufacturing approach. Unlike overmolding, which requires high tooling costs and secondary operations, ART enables direct integration of reinforcement with minimal additional processing. Similarly, compared to automated fiber placement, ART offers a cost-effective alternative for lightweight applications without the need for complex deposition systems. It has strong potential in sectors such as automotive, packaging, and consumer goods, where lightweighting and localized reinforcement are increasingly important.

Some previous studies have investigated overprinting of polymers such as polyamides [15, 16], acrylonitrile butadiene styrene [17] and polylactic acid [18] on polymer substrates. Nevertheless, there is still a notable gap in understanding the specific application of overprinting in thermoforming operation. This study addresses this gap by investigating the effect of processing conditions during overprinting of PETG/carbon fiber filament (PETG/CF) onto PETG sheet intended for ART. The mechanical properties of the additively reinforced ART materials were also evaluated. By leveraging AM technique to reinforce PETG with PETG/CF the neat polymer strength and rigidity were enhanced. The investigations carried out in this study also provided information that can aid the thermoforming process. Future studies are expected to uncover more insights that will drive advancements in ART technology, moving the industry toward higher levels of innovation and efficiency in manufacturing processes and material utilization.

2. Experimental techniques

The ART materials were produced using an ABB arm Orbital printer. The 1.5 mm thick PETG sheet was laid on a vacuum-assisted printing platform. Subsequently, the reinforcing composite (PETG/CF with 10 wt.% carbon fiber) was deposited (overprinted) onto the substrate polymer at 265 °C and 285 °C. These printing temperatures were selected to determine how changes in printing temperature influence the adhesion quality, material properties, and overall performance of the developed ART material. The printer maintained precise filament deposition along a predefined path, ensuring a controlled layer thickness of 0.5 mm and a bead width of 1.2 mm throughout the printing. The printing progresses layer by layer until the desired thickness (1.5 mm) was achieved, resulting in parts measuring 140 x 140 mm. As a reference, a 3 mm thick box measuring 140 x 140 mm was printed solely with PETG/CF at 265 °C and 285 °C to evaluate the printed structure properties. Table 1 provides information about the sample designations.

Table 1: Information about samples designation

Samples Designation*	Description
AM	
265x	PETG/CF printed at 265 °C and analyzed in x-direction relative to printing direction
265z	PETG/CF printed at 265 °C and analyzed in z-direction relative to printing direction
285x	PETG/CF printed at 285 °C and analyzed in x-direction relative to printing direction
285z	PETG/CF printed at 285 °C and analyzed in z-direction to printing direction
ART	
A265x	ART material produced at 265 °C and analyzed in x-direction relative to printing direction
A265z	ART material produced at 265 °C and analyzed in z-direction relative to printing direction
A285x	ART material produced at 285 °C and analyzed in x-direction relative to printing direction
A285z	ART material produced at 285 °C and analyzed in z-direction relative to printing direction

*The x-direction refers to the plane parallel to the printing surface and along the path of material deposition, while the z-direction represents the axis perpendicular to the printing layers, reflecting interlayer properties. ART- Additively Reinforced Thermoforming

2.1 Thermal, Thermomechanical, Mechanical, Microstructural, and Adhesive Strength Analyses

We characterized the materials using Differential Scanning Calorimetry (DSC) to evaluate the glass transition temperature (T_g) of the neat PETG sheet and the printed PETG/CF samples. This analysis provide insight into suitable thermoforming temperature, which is typically above the T_g but below the melting temperature. The measurement was conducted in a non-oxidizing environment using 100% nitrogen at a controlled flow rate of 50 cm^3/min (TA Instruments DSC 2500). Each sample were subjected to a sequential thermal cycle involving heating at 2 °C/min from ambient to 30 °C, holding for 2 minutes, and then heating to 300 °C.

Thermogravimetric analysis (TGA) was conducted to evaluate thermal degradation behavior, decomposition temperature, and overall thermal stability of those materials. Samples

were heated from 30 °C to 600 °C at 10 °C/min in an oxidizing environment (air) with a 50 cm^3/min flow rate (TA Instruments Q5500).

Heat deflection temperature under load measurements were conducted using a 3-point bending mode (TA Instruments DMA 850) (Figure 1a). Following ASTM D648 standard, a constant force of 0.7 N was applied, while the temperature was increased at a rate of 2 °C/min to 200 °C. Heat deflection temperatures of the analyzed samples were then determined from the resulting curves. The effect of varying load (0.1, 0.3, and 0.7 N) and heating rates (2, 3, and 5 °C/min) on the extent and pattern of deformation was also investigated. In each case, the experiment ended after reaching the maximum deformation capacity.

Tensile specimens were prepared from the 140 x 140 mm PETG/CF box, 3 mm thick PETG sheet and the developed ART sheets through waterjet cutting (Figure 1b). The samples were dried (Grieve oven) at 25 °C for 4 hours. The tensile testing was conducted according to ASTM D638 (Type IV) standards at a crosshead speed of 5 mm/min with a signal sampling rate of 10 Hz. An Instru-Met Floor Universal Tensile Testing Machine equipped with 5000 lbs load cell was utilized to assess the mechanical properties of the samples. To ensure results' accuracy and reliability, four repeatability tests were performed per each sample. The tensile strength (which correspond to the peak values at failure of the overprint layer for the ART material) and elastic modulus were measured in both the x and z-directions relative to printing direction. Regarding the ART material, the test was stopped when the reinforcing layer failed because the tensile stress dropped at this point while the substrate PETG continued to elongate until final failure. Moreover, the tensile properties of the PETG substrate were independently determined.

A Zeiss Axio Imager.M2m microscope was used to obtained optical images of the interface between the base polymer sheet and the reinforcing layer to investigate the quality and characteristics of the interfacial bond. The images were captured using a 2.5x lens across 8mm surface length.

A single lap shear strength (SLS) testing was employed to assess the interfacial strength between the overprint (PETG/CF) and substrate (PETG) materials. This assessment is important to ensure effective load transfer between the reinforcing layer and to ensure the structural integrity and functionality of the ART material. The measurements were carried out following ASTM D5868 standards using an Instru-Met Floor Universal Tensile Testing machine equipped with 5000 lbs load cell. PETG/CF was printed on top of two halves PETG sheets under similar conditions employed to manufacture the ART. To control adhesion, one of the sheets was entirely covered with Kapton tape, leaving only the lap region exposed to allow the reinforcing layer to bond. The PETG/CF was then overprinted across the top of both halves, as illustrated in Figure 1c. Subsequently, test samples were cut out using a waterjet cutting machine. The coupons were then dried in a Grieve oven at 25 °C for 8 hours before the test. The measurements were conducted at a pull rate of 13 mm/min with a replicate of four samples. The shear strength at failure was determined by dividing the maximum load at failure by the bonded area. The overprinting was also done on preheated PETG sheets at 55 °C to evaluate the impact of substrate preheating on adhesion between the reinforcing layer and substrate material.

Figure 1d shows the image of a part demonstrating the application of additive reinforcement in thermoforming application

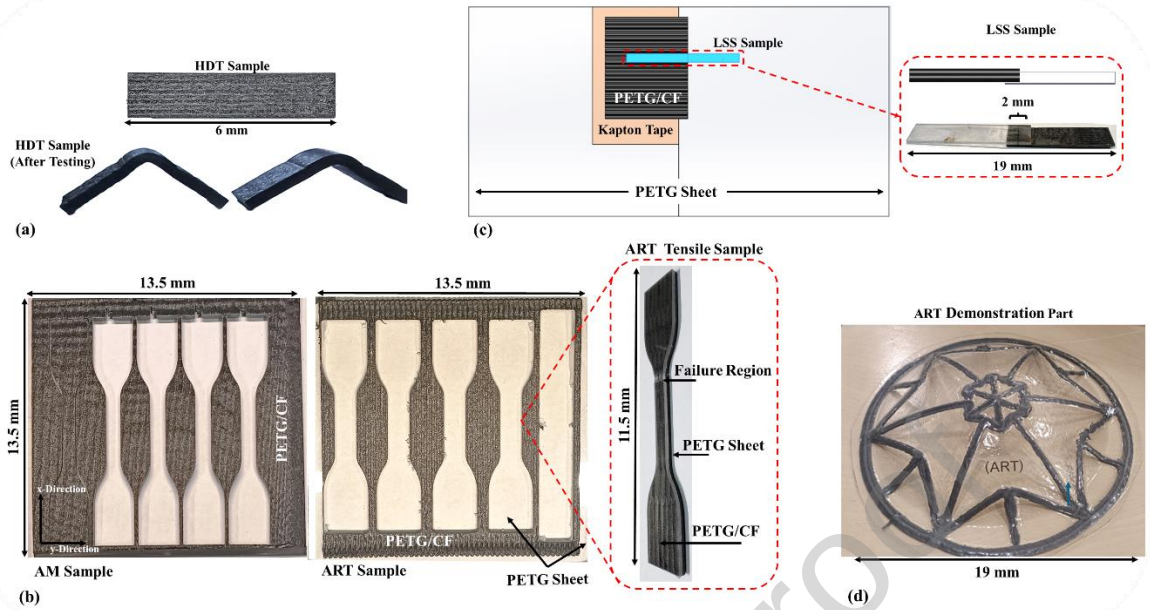

Figure 1: Images showing characterized samples and ART demonstration part: (a) HDT samples, (b) LSS sample and printing strategy, (c) PETG/CF and ART tensile samples, and (d) ART part [ART: Additive Reinforced Thermoforming; HDT: Heat Deflect Temperature; LSS: Lap Shear Strength]

3. Results and Discussion

3.1 Thermal and Thermomechanical Behavior of ART Materials and Their Components

The DSC curves for PETG sheet and PETG/CF printed at 265 °C and 285 °C are shown in Figure 2a. The T_g of the substrate and reinforcing layer was determined to be approximately 70 °C. This similarity in T_g offers benefits that include processing compatibility, uniform thermal behavior, minimized stress during bonding and improved bond strength. The exothermic peak at 220 °C was not detected when DSC measurement was conducted using a faster heating rate of 10 °C/min (Figure 2ai). This peak may be attributed to localized crystalline regions formed due to the slow heating rate during the DSC measurement. PET and PETG share similar chemical structures, with PETG being modified by the inclusion of glycol to reduce crystallinity and improve processing. However, under certain condition like a slow heating rate or inclusion of nucleating agent, PETG can exhibit a cold crystallization peak [19-22]. At the faster heating rate, the T_g also shifted to 120.3 °C. This upward shift in T_g is attributable to thermal lag and reduced relaxation time available for polymer chains to rearrange their molecular configurations as temperature increases rapidly [23, 24].

The thermogravimetric profiles, which offer valuable insights into the thermal responses of PETG sheet and PETG/CF samples, are shown in Figure 2b. Both the PETG sheet and PETG/CF samples exhibited a similar maximum degradation temperature of approximately 404 °C and 401 °C, respectively [1]. These values indicate that the selected printing temperatures did not degrade either material. The PETG/CF composite showed a better overall thermal stability compared to the PETG sheet due to the presence of carbon fiber. The reinforcing layer had a residual mass approximately 10% higher than the substrate material. Consequently, the ART materials would possess enhanced overall thermal stability compared to the individual base polymer. Moreover, changes in printing temperature did not have a

significant impact on the overall thermal stability of the PETG/CF. The TGA profiles align with existing literature that attributes the degradation mechanisms of PETG to chain scission and hydrolysis at elevated temperatures [25, 26].

The deformation pattern of PETG/CF under various conditions are shown in Figure 2c-2e. Under constant load (450 Pa/0.7 N), the deposition material exhibited successive heat deflection temperature points under load (DTUL) with increasing temperature (Figure 2c). This is due to increased molecular mobility of the polymer chains, which causes the material to undergo plastic deformation. Irrespective of the printing temperature, the PETG/CF starts to deform at ~70 °C until ~80 °C at which point the deformation pattern changes as the material developed decreased resistance to deformation. The onset of deformation corresponds to the T_g of the neat polymer and therefore can be associated with PETG (see the DSC curves). At this stage, the PETG sheet exhibited the lowest resistance to deformation, indicated by a displacement value of 2.44 mm at 74 °C, which is the end point of the initial deformation phase. Generally, polymer chains have increased mobility at higher temperatures, which allow them to rearrange and slide past one another more easily [27]. Above the T_g, the matrix soften significantly, facilitating a more rapid plastic flow, which enable the polymer to deform under applied stress as indicated in the curved profiles. By comparing the overall heat deflection curve of the PETG sheet and reinforicing layer, the former exhibited increased deformation under similar conditions. Considering sustained maximum deformation temperature, the reinforced layer can withstand deformation at a temperature 14.7°C higher than the neat polymer, representing a 14.1% increase. The increased resistance to deformation by the reinforcing layer can be attributed to the presence of carbon fiber, which provided a higher stiffness. This is beneficial to the ART material considering the need for deep draw during thermoforming and improved rigidity of parts. The sequential pattern of the DTUL curves arises from the viscoelastic nature of the polymer matrix and contributory effect of the carbon fiber. This characteristic can influence the choice of forming temperatures, heating rate, and cooling processes. Understanding these properties will help to tailor the thermoforming parameters (heating and cooling rate) to ensure the thermoforming operation is carried out at a temperature that promote sustained deformation under specific thermoforming conditions. Similar to earlier observation, the printing temperature did not t have a significant impact on the deformation pattern (see Figure 2b).

The effect of varying load and heating rate on the heat deflection temperature curve was investigated using PETG/CF produced with a printing temperature of 265 °C. The resulting curves are shown in Figure 2d and 2e. Figure 2d shows the effect of load on the deformation of the PETG/CF under increasing temperature. The initial maximum deformation temperature changes from 88 °C to 70 °C and 73 °C as the load increased from 0.1 N to 0.3 N and 0.7 N, respectively. This represent a decreased by 20.45% and 17.05% when the load increased from 0.1 N to 0.3 N and 0.7 N, respectively. The observed decrease in the maximum deformation temperature with increasing load is due to stress-induced enhancement of molecular mobility within the polymer chain. The increased stress can induce chain relaxation, making the chains more mobile at lower temperatures. Overall, the curve shows that actual forming temperature and process time will depend on pressure (applied vacuum) during thermoforming. The lower the vacuum pressure, the higher the forming temperature and process time that will be required. Moreover, the investigated heating rates do not have any significant effect on the onset of deformation but still influence the overall deformation pattern (Figure 2e). Generally, the temperature at which sustained deformation occurs increased with increasing heating rate. The temperatures for sustained maximum deformation are 143.1°C, 148.3 °C, and 163.5 °C for heating rates of 2°C/min, 5°C/min, and 10°C/min, respectively. Consequently, both the vacuum pressure and heating rate should be optimized to attain good formability. This results agrees

with the observation by Leite et al. [28] that heating time and heating power are significant factors in vacuum thermoforming.

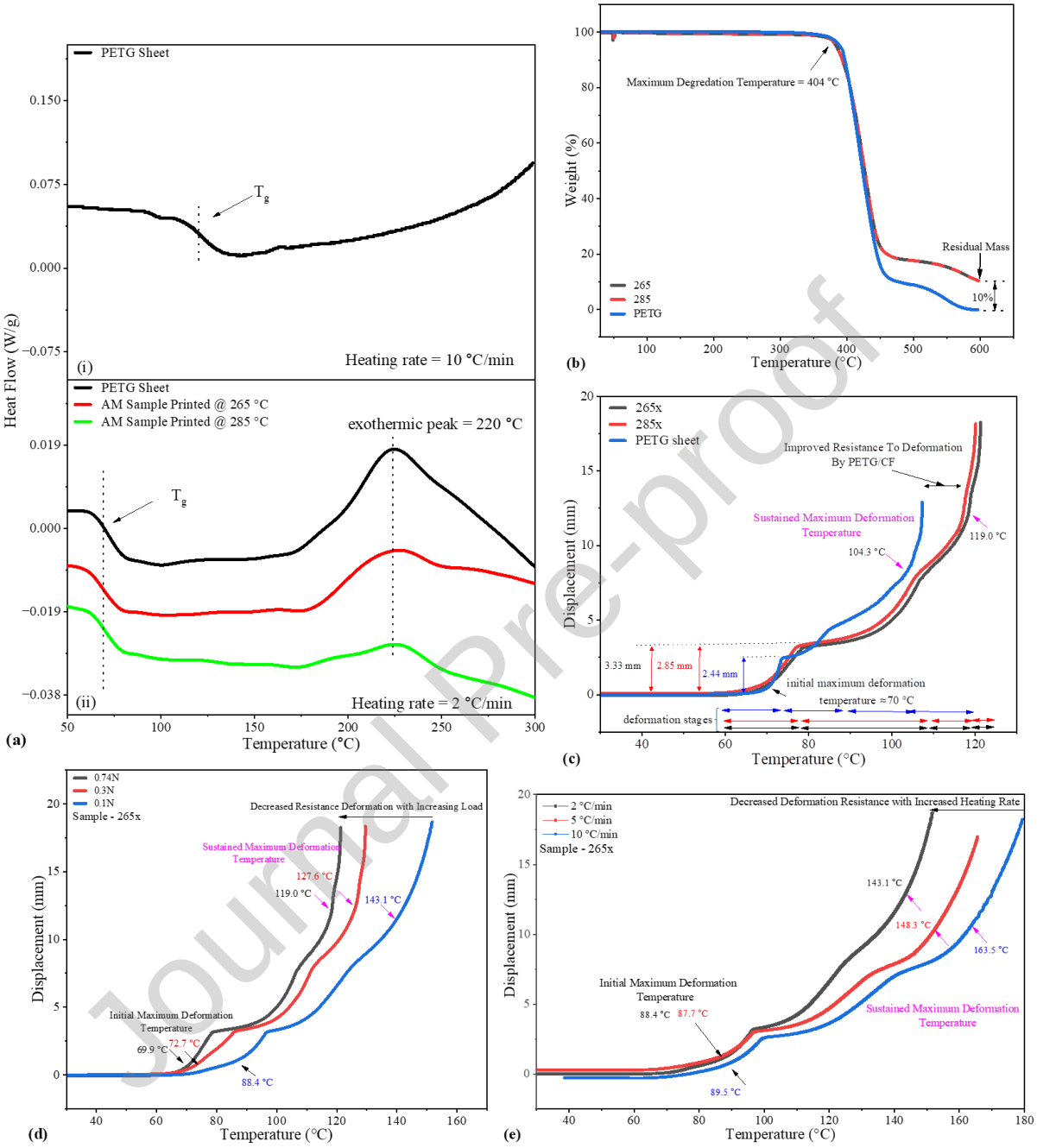

Figure 2: Thermal and thermomechanical analysis of PETG and PETG/CF composites: (a) DSC curves of PETG sheet, PETG/CF printed at 265 °C and 285 °C; (b) Thermogravimetric profiles of PETG sheet, PETG/CF printed at 265 °C and 285 °C; (c-e) Heat deflection behavior of PETG sheet and8 printed PETG/CF: (c) Comparison of PETG sheet vs PETG/CF printed at different temperatures, (d) Effect of varying load at a constant heating rate of 2 °C/min, and (e) Effect of varying heating rate at a constant load of 1 °C/min.

3.2 Mechanical Properties and Interfacial Characteristics

The tensile strength and modulus of elasticity of the PETG/CF (overprint material), PETG sheets (base polymer), and ART materials were determined in both the x and z-directions (Figure 3).

The overprint material produced at 265 °C has a tensile strength of 68.1 ± 1.9 MPa in the x-direction, whereas the sample produced at 285 °C exhibited a higher value of 73.9 ± 1.1 MPa (Figure 3a). The results showed that increased printing temperature favored improved tensile strength by 8.5%. In the z-direction, the tensile strength values were 16.2 ± 2.1 MPa and 20.2 ± 2.1 MPa relative to the printing temperature of 265 °C and 285 °C, respectively. This observation remains consistent regardless of the testing direction. Compared to these values, the tensile strength of the neat polymer was 49.1 ± 0.5 MPa, which is approximately 35.1% and 31.1% lower than the overprint material produced at 265 °C and 285 °C, respectively. These results align with previous studies that higher printing temperatures can enhance fluidity, fusion, and interlayer bonding, which is favorable to improved strength [29, 30].

The modulus of elasticity in the x-direction of the overprint material was higher than that of the PETG sheet (1.92 ± 0.09 GPa). The PETG/CF produced at 265°C and 285°C exhibited increases of 295% and 257%, respectively (Figure 3f). In the x-direction, rigidity decreased with increasing printing temperature, dropping from 7.59 ± 0.34 GPa to 6.86 ± 0.67 GPa [31]. This can be attributed to the observed increased in porosity of PETG/CF at higher printing temperature (see Figure 3f). Porosity can significantly disrupt continuous load transfer within the material, reducing its stiffness [32]. In the z-direction, a slight increase in material stiffness was also observed relative to the neat PETG. At this instance, the modulus of elasticity increased with higher printing temperatures, rising from 2.45 ± 0.29 GPa to 2.59 ± 0.16 GPa.

Figure 3c shows the tensile strength of the ART materials (1.5 mm thick polymer sheet and 1.5 mm thick reinforcing layers) produced by overprinting the composite material on PETG sheets. The tensile strength in the x-direction of the additively reinforced PETG sheet was higher than the equivalent neat 3 mm sheet (49.1 ± 0.5 MPa). The tensile strength values correspond to 57.32 ± 2.9 MPa and 53.18 ± 2.48 MPa for the ART material produced at 265 °C and 285 °C, respectively. A significant increase in modulus of elasticity was observed in the x-direction for the overprint material compared to the neat PETG (1.92 ± 0.09 GPa). The 265x and 285x samples exhibited moduli of elasticity of 3.41 ± 0.4 GPa and 3.53 ± 0.06 GPa, respectively, representing increases of approximately 78% and 84%. The reinforcing layer of the 285°C ART material exhibited higher porosity, while the substrate layer, produced at 265°C, showed a higher degree of porosity, suggesting that off-gassing from the substrate material may be a contributing factor to porosity formation, particularly at higher temperatures [33]. For the developed ART material, the slight decrease in tensile strength can be attributed to increased porosity in the reinforcing. The optical microscope images also show good interfacial bonding between the reinforcing layer and substrate polymer. There was unidentifiable transition between both materials, which suggest the existence of a good fusion/bonding between the PETG sheet and the overprinted PETG/CF.

The SLS remained consistent for both 265x and 285x samples, regardless of whether the sheet was preheated or not (Figure 3f). The SLS was approximately 7.5 MPa for 265x and 7.8 MPa for 285x samples. These results indicate that the investigated printing temperatures had no significant impact on interfacial strength between layers. Similar results were obtained for the tensile properties with no significant difference in performance regardless of preheating the sheet before overprinting. The lack of significant effect of preheating the sheet may be attributed to the relatively low preheating temperature (55 °C), which is below the sheet's glass transition temperature (70 °C). While preheating above T_g could potentially enhance interfacial bonding by increasing molecular mobility, it may also introduce challenges such as sheet warping and loss of dimensional stability during printing [34]. 3.60 ± 0.33 GPa and 3.35 ± 0.07 GPa.

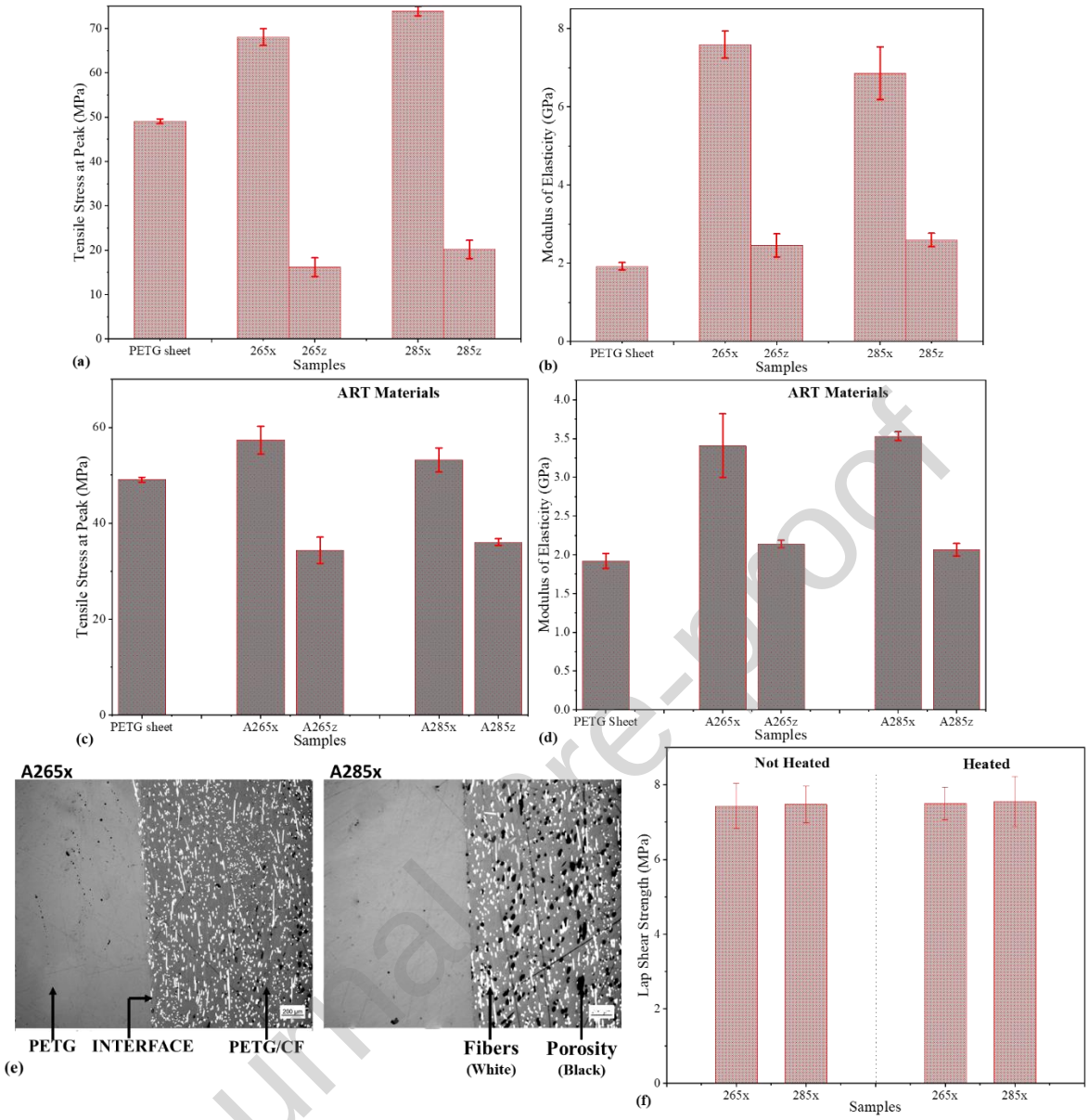

Figure 3: (a) Tensile strength of the unreinforced PETG sheet and PETG/CF materials, (b) Modulus of elasticity of the unreinforced PETG sheet and PETG/CF materials, (c) Tensile strength of the overprinted PETG ART materials, (d) Modulus of elasticity of the ART materials, and (e) Lap shear strength of the ART materials as a function of processing parameters. (f) Microstructure of the ART material produced at 265 °C and 285 °C, showing good interfacial bonding between the base polymer sheet and the reinforcing layer. [ART: Additive Reinforced Thermoforming]

4. Conclusion

In this study, PETG sheets were additively reinforced with PETG/CF for application in thermoforming operation. The investigated properties provided insights into the materials' thermal stability, deformation behavior, viscoelasticity, mechanical performance, and interfacial adhesion. In the x-direction, the tensile strength of PETG/CF increased with printing

temperature, reaching 68.1 MPa at 265°C and 73.9 MPa at 285°C, which is significantly higher than the tensile strength of neat PETG (49.1 MPa). In the z-direction, tensile strength rose from 16.2 MPa to 20.2 MPa with increasing printing temperature. Compared to neat PETG (which has a modulus of elasticity of 1.92 ± 0.09 GPa), the modulus of elasticity of the overprint material increased significantly in the x-direction, exhibiting increases of 295% and 257% for the PETG/CF produced at 265°C and 285°C, respectively. A slight increase in stiffness was also observed in the z-direction, rising from 2.45 to 2.59 GPa with higher printing temperatures. The improvement in materials properties of the reinforcing layer was translated to the significant performance of the ART material relative to the neat PETG. The ART materials demonstrated an improved tensile strength (up to 57.32 MPa), representing a 16.74% increase, and a significantly improved stiffness (up to 3.60 GPa), representing an 87.50% increase. Interfacial strength, as evidenced by lap shear strength values around 7.5 MPa and 7.8 MPa for both 265x and 285x samples, respectively, was not significantly influenced by preheating or printing temperatures. These results show ART's potential to enhance thermoformable substrates, enabling lightweight, high-performance components with improved strength, stiffness, and stability over neat thermoplastics.

Acknowledgments

The authors gratefully acknowledge support from the U.S. Department of Energy, Advanced Materials and Manufacturing Technologies Office under contract DE-AC05-00OR22725 with UT-Battelle, LLC.

Data availability statement

The data supporting the findings of this study are available from the corresponding author upon request.

References

1. Liao, X., et al. *The thickness and gap width of aligners made of three types of thermoforming materials: An in-vitro study*. in *Seminars in Orthodontics*. 2024. Elsevier.
2. Matsuda, A., et al., *Evaluation of mechanical tests conducted before and after thermoforming of aligners.* The Showa University Journal of Medical Sciences, 2023. **35**(3): p. 121-130.
3. Stack, R.M. and F. Lai, *Development in thermoforming thermoplastic composites.* Thermoforming Quarterly, 2013. **32**: p. 48-53.
4. Yi, N., et al., *Correlation between interfacial bond strength and degree of healing in overprinting PAEK on CF/PAEK composites.* Composites Part A: Applied Science and Manufacturing, 2024: p. 108217.
5. Donderwinkel, T., M. van Drongelen, and S. Wijskamp. *Strength Development in Overmolded Structures*. in *Advances in Polymer Processing 2020*. 2020. Berlin, Heidelberg: Springer Berlin Heidelberg.
6. Zhao, Z., et al., *Study on the Overmolding Process of Carbon-Fiber-Reinforced Poly (Aryl Ether Ketone) (PAEK)/Poly (Ether Ether Ketone) (PEEK) Thermoplastic Composites.* Materials (Basel), 2023. **16**(12).

7. Stewart, R., *Thermoplastic composites — recyclable and fast to process.* Reinforced Plastics, 2011. **55**(3): p. 22-28.
8. El Hawary, O., et al. *An Overview of Natural Fiber Composites for Marine Applications*. Journal of Marine Science and Engineering, 2023. **11**, DOI: 10.3390/jmse11051076.
9. Yao, S.-S., et al., *Recent advances in carbon-fiber-reinforced thermoplastic composites: A review.* Composites Part B: Engineering, 2018. **142**: p. 241-250.
10. Kanishka, K. and B. Acherjee, *Revolutionizing manufacturing: A comprehensive overview of additive manufacturing processes, materials, developments, and challenges.* Journal of Manufacturing Processes, 2023. **107**: p. 574-619.
11. Wong, J., A. Altassan, and D.W. Rosen, *Additive manufacturing of fiber-reinforced polymer composites: A technical review and status of design methodologies.* Composites Part B: Engineering, 2023. **255**: p. 110603.
12. Morales, U., et al., *Over-3D printing of continuous carbon fibre composites on organo-sheet substrates.* AIP Conference Proceedings, 2019. **2113**(1): p. 020015.
13. Rahmatabadi, D., et al., *Poly(ethylene terephthalate) glycol/carbon black composites for 4D printing.* Materials Chemistry and Physics, 2024. **325**: p. 129737.
14. Rahmatabadi, D., et al., *4D printing and annealing of PETG composites reinforced with short carbon fibers.* Physica Scripta, 2024. **99**.
15. Janssen, H., T. Peters, and C. Brecher, *Efficient Production of Tailored Structural Thermoplastic Composite Parts by Combining Tape Placement and 3d Printing.* Procedia CIRP, 2017. **66**: p. 91-95.
16. Holzinger, M., et al., *New additive manufacturing technology for fibre-reinforced plastics in skeleton structure.* Journal of Reinforced Plastics and Composites, 2018. **37**(20): p. 1246-1254.
17. Pierson, H.A. and B. Chivukula, *Process–Property Relationships for Fused Filament Fabrication on Preexisting Polymer Substrates.* Journal of Manufacturing Science and Engineering, 2018. **140**(8).
18. Boros, R., P.K. Rajamani, and J.G. Kovacs, *Combination of 3D printing and injection molding: Overmolding and overprinting.* Express Polymer Letters, 2019. **13**(10).
19. Kichloo, A.F., et al., *Impact of Carbon Fiber Reinforcement on Mechanical and Tribological Behavior of 3D-Printed Polyethylene Terephthalate Glycol Polymer Composites—An Experimental Investigation.* Journal of Materials Engineering and Performance, 2022. **31**(2): p. 1021-1038.
20. Valvez, S., A.P. Silva, and P.N.B. Reis, *Optimization of Printing Parameters to Maximize the Mechanical Properties of 3D-Printed PETG-Based Parts.* Polymers (Basel), 2022. **14**(13).
21. Chen, T. and J. Zhang, *Non-isothermal cold crystallization kinetics of poly(ethylene glycol-co-1,4-cyclohexanedimethanol terephthalate) (PETG) copolyesters with different compositions.* Polymer Testing, 2015. **48**: p. 23-30.
22. Garwacki, M., et al., *The Development of Sustainable Polyethylene Terephthalate Glycol-Based (PETG) Blends for Additive Manufacturing Processing-The Use of Multilayered Foil Waste as the Blend Component.* Materials (Basel), 2024. **17**(5).
23. Thomas, L.C., *Use of multiple heating rate DSC and modulated temperature DSC to detect and analyze temperature-time-dependent transitions in materials.* American Laboratory, 2001. **33**: p. 26+28+30-31.
24. Yong, A.X.H., et al., *Heating rate effects on thermal analysis measurement of Tg in composite materials*. Advanced Manufacturing: Polymer & Composites Science, 2017. **3**(2): p. 43-51.

25. Venkatachalam, S., et al., *Degradation and Recyclability of Poly (Ethylene Terephthalate)*, in *Polyester*, M.S. Hosam El-Din, Editor. 2012, IntechOpen: Rijeka. p. Ch. 4.
26. Latko-Durałek, P., K. Dydek, and A. Boczkowska, *Thermal, Rheological and Mechanical Properties of PETG/rPETG Blends.* Journal of Polymers and the Environment, 2019. **27**(11): p. 2600-2606.
27. Fenimore, L.M., M.J. Suazo, and J.M. Torkelson, *Covalent Adaptable Networks Made by Reactive Processing of Highly Entangled Polymer: Synthesis-Structure-Thermomechanical Property-Reprocessing Relationship in Covalent Adaptable Networks.* Macromolecules, 2024. **57**(6): p. 2756-2772.
28. Leite, W.D., et al. *Vacuum Thermoforming Process: An Approach to Modeling and Optimization Using Artificial Neural Networks*. Polymers, 2018. **10**, DOI: 10.3390/polym10020143.
29. Hadi, A., A. Kadauw, and H. Zeidler, *The effect of printing temperature and moisture on tensile properties of 3D printed glass fiber reinforced nylon 6.* Materials Today: Proceedings, 2023. **91**: p. 48-55.
30. Hsueh, M.H., et al., *Effect of Printing Parameters on the Thermal and Mechanical Properties of 3D-Printed PLA and PETG, Using Fused Deposition Modeling.* Polymers (Basel), 2021. **13**(11).
31. Magri, A.E., et al., *Printing temperature effects on the structural and mechanical performances of 3D printed Poly-(phenylene sulfide) material.* IOP Conference Series: Materials Science and Engineering, 2020. **783**(1): p. 012001.
32. Ashebir, D.A., et al., *Detecting Multi-Scale Defects in Material Extrusion Additive Manufacturing of Fiber-Reinforced Thermoplastic Composites: A Review of Challenges and Advanced Non-Destructive Testing Techniques.* Polymers (Basel), 2024. **16**(21).
33. Talabi, S.I., et al., *Fiber orientation and porosity in large-format extrusion process: The role of processing parameters.* Composites Part A: Applied Science and Manufacturing, 2025. **194**: p. 108891.
34. Kishore, V., et al., *Infrared preheating to improve interlayer strength of big area additive manufacturing (BAAM) components.* Additive Manufacturing, 2017. **14**: p. 7-12.

Graphical abstract

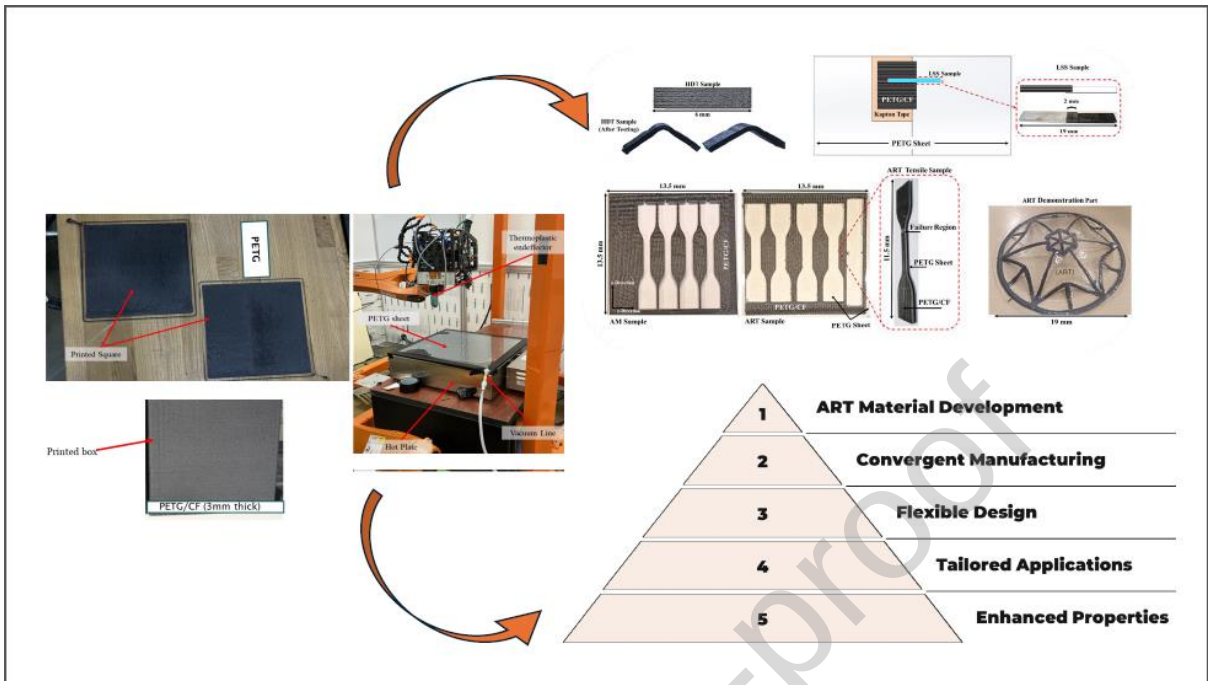

Declaration of interests

☒ The authors declare that they have no known competing financial interests or personal relationships that could have appeared to influence the work reported in this paper.

☐The authors declare the following financial interests/personal relationships which may be considered as potential competing interests: